Classification of heat transfer regimes of saturated droplets impinging on heated surface

Junseok Park [a], Hongdae Yu [a], Hyungdae Kim [a*]
[a]*Nuclear Engineering department, Kyung Hee University, Youngin, Republic of Korea*
[*]*Corresponding author: hdkims@khu.ac.kr*

1. Introduction

During a large break loss of coolant accident (LOCA) in a pressurized water nuclear reactor, the collision heat transfer of saturated droplets above Leidenfrost point temperature [1] is of great importance in predicting the peak cladding temperature of overheated fuel rods. Under LOCA conditions, the Weber number of droplets is expected to be less than 30 which implies that the impact regime is a perfect rebound without atomization of the small droplet [2].

Behaviors of droplet show different physical aspects according to the temperature of the materials during impinging of droplet on a heated wall. Early studies focused on the dynamic characteristics because of the difficulty of measuring the heat transfer characteristics of colliding droplet. Some studies [3-12] have determined the regime maps based on dynamic characteristics such as rebound, splash, and break-up. For example, Tran [12] suggested heat transfer regime of subcooled droplets colliding with a heated surface only based on collision dynamics. They considered the heat transfer regime of the bouncing droplet to be the film boiling.

So far, a common issue with heat transfer regime map is that it is inherently qualitative by exploiting the dynamic behaviors of droplet, not based on quantitative value of heat transfer. Our group investigated and found that the heat transfer characteristics of a saturated bouncing droplet could vary even though the dynamic behaviors are similar, as shown in Fig. 1 [13]. This result shows that an identification for heat transfer regimes of droplet impinging on heated surface is not yet clear.

Therefore, this study aims to experimentally determine a heat transfer regime map solely based on quantitative heat transfer amount instead of qualitative observation of collision dynamics.

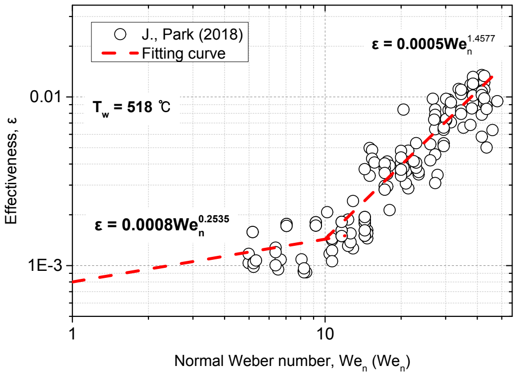

Fig. 1. Heat transfer effectiveness of a saturated bouncing droplet per a collision as a function of Weber number [13]

2. Experiments

2.1 Experimental setup

Fig. 2 shows the experimental setup for the droplet-wall collision test. Collision dynamics and associated heat transfer characteristics of a saturated droplet colliding onto a hot Sapphire plate at various collision velocities and surface temperature are examined using synchronized high-speed video (Phantom v7.3) and infrared cameras (FLIR SC6000) with a frame rate of 1.5 kHz.

The droplet-wall collision interface temperature was measured using the infrared camera. The combination of the infrared-opaque Pt film on the infrared-transparent sapphire permits to measure surface temperature of the 100-nm-thickness Pt film from below of the sapphire test sample.

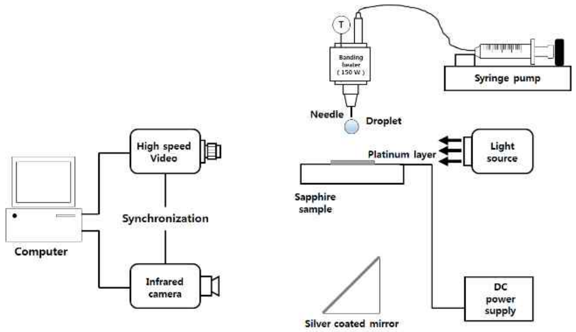

Fig. 2. Schematic of the experimental apparatus [14]

2.2 Experimental conditions

Table 1 summarizes the experimental conditions based on typical conditions of reflooding phase. In this study, deionized water was used as the working fluid in experiments.

Table. 1 Experimental conditions

Parameters	Experiments
Pressure [MPa]	0.1
Droplet temperature, T_d [℃]	100
Normal Weber number, We_n	2 - 46
Droplet diameter, D_d [mm]	1.7
Normal velocity, V_n [m/s]	0.2 – 1.3
Wall temperature, T_w [°C]	375 – 575

2.3 Data reduction

The heat transfer regimes are determined on the basis of the change in heat flux distribution and effectiveness. The important parameters in calculating the total heat transfer amount for a single droplet collision (E_d) are the effective heat transfer area and local heat flux distribution. The surface heat flux distribution was obtained by solving transient heat conduction equation for the heated substrate using the measured surface temperature data as the boundary condition of the collision surface [13]. Effective heat transfer area during droplet-wall interaction was defined using the local heat flux distribution. E_d was obtained by integrating the local heat flux obtained from the temperature distribution measured by the infrared camera over the residence time obtained by HSV. Finally, effectiveness (ε) is calculated by the ratio of the removed energy (E_d) during a droplet-wall collision to the energy (E_{max}) required to evaporate the droplet completely.

$$E_d = \int_{t_R} q'_w(t)A(t)dt \tag{1}$$

$$\boldsymbol{\varepsilon} = \frac{\boldsymbol{E_d}}{\boldsymbol{E_{m\,ax}}} = \frac{\boldsymbol{E_d}}{\boldsymbol{\rho_f \frac{\pi D_d^3}{6} h_{fg}}} \tag{2}$$

3. Results and Discussions

Heat transfer characteristics of droplets colliding with the heated wall are classified into two: film boiling and transition boiling. Fig. 3(a) shows images of the film boiling regime. The formed vapor film is thick enough to prevent the direct contact between the droplet and heated wall. Transition boiling is shown in Fig. 3(b). It is similar to the film boiling regime, but the droplet partially makes contact with the heated wall during collision process. The partial contact is due to higher inertial force of colliding droplets. It is found that transition boiling occurred at the high collision velocity and low surface temperature.

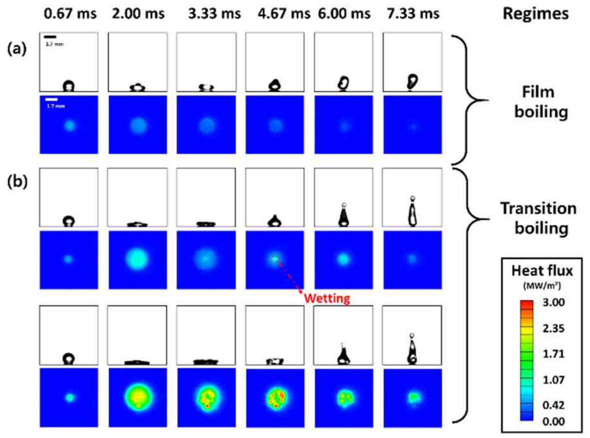

Fig. 3. Heat transfer regimes of saturated droplet: (a) Film boiling, (b) Transition boiling

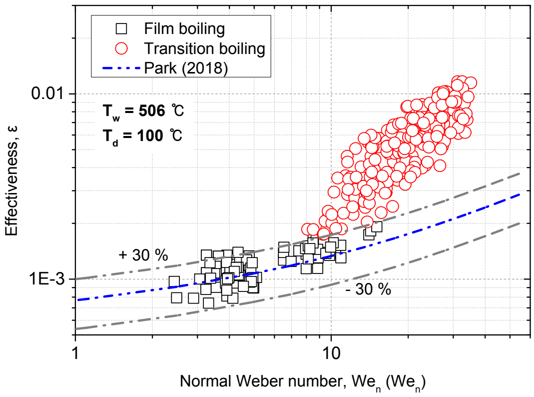

(a) 506 °C

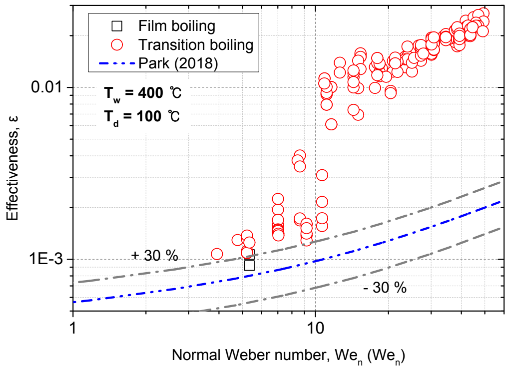

(b) 400 °C

Fig. 4. Effectiveness in accordance with collision velocity

Effectiveness of droplet-wall collision heat transfer calculated by integrating local surface heat flux is shown in Fig. 4. The heat transfer characteristics in the region where We_n is lower than 10 at 506 °C can be considered as film boiling regime. This is in agreement with magnitude of results during film boiling by Kendall and Rhosenow [15]. Experimental results considered as the film boiling are in good agreement with the prediction results using the heat transfer model.

However, the slope of the effectiveness at 506 °C changes due to the heat transfer enhancement by direct contacts occurring at the $We_n \geq 10$, as seen in Fig. 3(b). As the collision velocity increases, the heat transfer regime changes from film boiling to transition boiling. This may be because the inertial force of the droplet pushing the steam increases, which makes contact easier.

Fig. 4(b) shows the results obtained at 400°C. The overall trend of effectiveness as a function of the normal Weber number is similar to that at 506°C. However, the effectiveness at 400°C increases rapidly in the conditions of $We_n < 10$ and then gradually increased with increasing collision velocity. In addition, it shows that the experimental results are higher than the prediction results in the experimental range of present study.

Comparing the tendency of effectiveness at 400 °C to that of 506 °C, the difference in effectiveness would have been caused by the wall temperature. When the wall temperature is higher than the Leidenfrost temperature, the vapor film formed by the heat transfer prevents the direct contact of droplet on heated wall. On the other hand, the decrease of wall temperature results in the inhibition of vapor formation causing partial contact. These characteristics indicate the cause of the higher experimental results with respect to prediction results.

The regime map for saturated droplet-wall collision is constructed by a combination of surface temperature and normal Weber number, as shown in Fig. 5. It is found that film boiling occurred at the low collision velocity and high surface temperature. The transition between the film boiling and transition boiling regimes was related closely to the dynamic Leidenfrost temperature that depended on the collision velocity. The formation of vapor pressure corresponding to the dynamic pressure of droplet is required to maintain the film boiling regime. Therefore, a higher surface temperature is required to maintain the film boiling during the collision of droplet with high collision velocity on the heated surface [14].

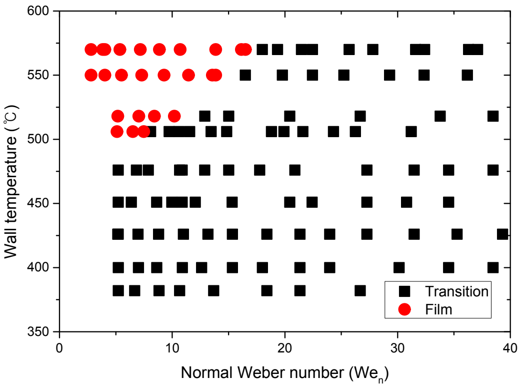

Fig. 5. Heat transfer regime map of saturated droplet

4. Conclusions

In this paper, heat transfer regimes of saturated droplet impinging on heated surface were experimentally investigated using the infrared thermometry technique. The regimes of saturated droplet are displayed on a quantitative two-dimensional map, having the initial surface temperature and the normal Weber number as coordinates.

Two distinct heat transfer regimes were identified during droplet-wall collision under reflooding phase conditions: film boiling and transition boiling. It is found that, although the collision behaviors is similar regardless of experimental conditions, the heat transfer characteristics of droplet change with the combined effect of collision velocity and wall temperature. This result indicates that the use of criteria based on dynamic characteristics makes a significant error when determining the classification of heat transfer regimes.

Therefore, it is essential to determine the heat transfer regimes of droplets based on a quantitative heat transfer amount. The regime map of a saturated droplet determined in this study will contribute to more accurate analysis of droplet-wall direct collision heat transfer in dispersed flow film boiling.

ACKNOLEDGEMENT

This work was supported by the National Research Foundation of Korea (NRF) grant funded by the Korean government (MSIP: Ministry of Science, ICT and Future Planning) (No. NRF-2015M2B2A9031597).

REFERENCES

[1] J.G. Leidenfrost, A tract about some qualities of common water, International Journal of Heat mass transfer, Vol.9, pp.1153-1166, 1966.

[2] L.H.J. Whachter and N.A.J. Westerling, The heat transfer from a hot wall to impinging water drops in the spheroidal state, Chemical Engineering Science, Vol.21, No.11, pp. 1047-1056, 1966.

[3] J.D. Bernardin, C.J. Stebbins and I. Mudawar, Mapping of impact and heat transfer regimes of water drops impinging on a polished surface, Int. J. Heat Mass Transfer, Vol.40, No. 2, pp.247-267, 1997.

[4] A.B. Wang, C.H. Lin and C.C. Chen, The critical temperature of dry impact for tiny droplet impinging on a heated surface, Vol.12, No. 6, pp.1622 - 1625, 2000.

[5] S.Y. Lee and S.U. Ryu, Recent progress of spray-wall interaction research, Journal of Mechanical science and technology, Vol.20, No. 8, pp.1101-1117, 2006.

[6] K. Black and V.Bertola, Drop impact morphology on heated surfaces, DIPSI Workshop 2012 on droplet impact phenomena & Spray investigation, May 18, Bergamo, Italy, pp.6-10, 2012.

[7] H.J.J. Staat, T. Tran, B. Geerdink, G. Riboux, C. Sun, J.M. Gordillo and D. Lohse, Phase diagram for droplet impact on superheated surfaces, Journal of fluid mech., Vol.779, R3, 2015.

[8] V. Bertola, An impact regime map for water drops impacting on heated surfaces, International journal of heat and mass transfer, Vol.85, pp.430-437, 2015.

[9] G. Liang, S. Shen, Y. Guo and J. Zhang, Boiling from liquid drops impact on a heated wall, international journal of heat and mass transfer, Vol. 100, pp.48-57, 2016.

[10] M. Shirota, M.A.J. van Limbeek, C. Sun, A. Prosperetti, and D. Lohse, Dynamic Leidenfrost effect: Relevant Time and Length scales, Physical review letters, Vol.116, 064501, 2016.

[11] H. Jadidbornab, I. Malgarinos, I. Karathanassis, N. Mitroglou and M. Gavaises, We-T classification of diesel fuel droplet impact regimes, Proceedings of the Royal society A, 4135049, 2018.

[12] T. Tran, H.J.J. Staat, A. Prosperetti, C. Sun, and D. Lohse, Drop impact on superheated surfaces, Physical review letters, Vol.108, 03101, 2012.

[13] Park, Experimental study on single droplet-wall collision heat transfer in film boiling, Thesis for degree of doctor of philosophy, 2018.

[14] J. Park and H. Kim, An experimental investigation on dynamics and heat transfer associated with a single droplet impacting on a hot surface above the Leidenfrost point temperature, kerntechnik, Vol.81, No.3, pp.233-243, 2016.

[15] G. E. Kendall and W. M. Rohsenow, Heat transfer to impacting drops and post critical heat flux dispersed flow, Technical report No.85694-100, Department of mechanical engineering, Massachusetts Institute of Technology, 1978.